Bell Aerospace TEXTRON

Niagara Frontier Operations
Bell Aerospace Textron
Division of Textron Inc.

Post Office Box One
Buffalo, New York 14240
716/297-1000

NASTRAN FORCED VIBRATION ANALYSIS OF

ROTATING CYCLIC STRUCTURES

by

V. Elchuri

Principal Engineer, Structural Dynamics

G. C. C. Smith

Chief Engineer, Structural Dynamics

A. Michael Gallo

Senior Programmer, Data Processing - Software Engineering

BELL AEROSPACE TEXTRON

Buffalo, N.Y. 14240

ABSTRACT

Theoretical aspects of a new capability developed and implemented in NASTRAN Level 17.7 to analyze forced vibration of a cyclic structure rotating about its axis of symmetry are presented. Fans, propellers, and bladed shrouded discs of turbomachines are some examples of such structures. The capability includes the effects of Coriolis and centripetal accelerations on the rotating structure which can be loaded with:

1) directly applied loads moving with the structure and

2) inertial loads due to the translational acceleration of the axis of rotation ('base' acceleration).

Steady-state sinusoidal or general periodic loads are specified to represent:

1) the physical loads on various segments of the complete structure, or

2) the circumferential harmonic components of the loads in (1).

The sinusoidal loads are specified as functions of frequency and the general periodic loads are specified as functions of time. The translational acceleration of the axis of rotation is specified as a function of frequency in an inertial coordinate system.

The cyclic symmetry feature of the rotating structure is used in deriving and solving the equations of forced motion. Consequently, only one of the cyclic sectors is modelled and analyzed using finite elements, yielding substantial savings in the analysis cost. Results, however, are obtained for the entire structure. A tuned twelve-bladed disc example is used to demonstrate the various features of the capability.

1. INTRODUCTION

Under the sponsorship of NASA's Lewis Research Center, a series of new capabilities has been developed and added to the general-purpose finite-element structural-analysis program NASTRAN [1-7]. A variety of problems including static aerothermoelastic and dynamic aeroelastic analyses of tuned cyclic structures, and modal analysis of mistuned cyclic structures, such as bladed discs of turbomachines, and advanced turbopropellers have been addressed. This paper presents the theoretical aspects of one of these NASTRAN capabilities [4,5].

Figure 1 illustrates the problem by considering a 12-bladed disc as an example. The bladed disc consists of twelve 30° segments--identical in their geometric, material and constraint properties. The disc rotates about its axis of symmetry at a constant angular velocity. The axis of rotation itself is permitted to oscillate linearly in any given inertial reference. In addition, the bladed disc is allowed to be loaded with steady sinusoidal or general periodic loads moving with the structure. Under these conditions, it is desired to determine the dynamic response (displacement, acceleration, stress, etc.) of the bladed disc.

2. EQUATIONS OF MOTION

The cyclic symmetry feature of the rotating structure is utilized in deriving and solving the equations of forced motion. Consequently, only one of the cyclic sectors is modelled and analyzed using finite elements, yielding substantial savings in the analysis cost. Results, however, are obtained for the entire structure. The Coriolis and centripetal acceleration terms have been included. For clarity of derivation, the equations of motion are first derived for an arbitrary grid point of the cyclic sector finite element model, and then extended for the complete model.

COORDINATE SYSTEMS

These are shown in Figure 1. O-XYZ is an inertial coordinate system. O-$X_B Y_B Z_B$ is a body-fixed coordinate system such that OX_B coincides with the axis of rotation of the structure and is always parallel to OX. For a NASTRAN finite element model of the bladed disc, O-$X_B Y_B Z_B$ also represents the Basic coordinate system. A-xyz is a body-fixed global coordinate system in which the displacements of any grid point P are desired. The unit vectors associated with these coordinate systems are also shown in Figure 1.

DEGREES OF FREEDOM

The rotating structure is permitted four rigid body motions including three translations (along OX, OY and OZ) and one rotation at a constant angular velocity Ω about its axis of rotation OX_B.

Each grid point of the structure is permitted six degrees of freedom. The displacement at any grid point in any sector can be expressed in any body-fixed coordinate system as a combination of:

1) the steady state displacement due to the steady rotation of, and the steady state loads applied to, the structure, and

2) the vibratory displacement (superposed on the steady displacement) due to the vibratory excitation provided by the directly applied loads and the inertial loads due to the acceleration of the axis of rotation ('base' acceleration).

The purpose of the present development is to determine the vibratory response.

LAGRANGE FORMULATION

Referring to Figure 1 , the complete <u>tuned</u> structure consists of N <u>identical</u> cyclic sectors. If u represents all the vibratory degrees of freedom of the <u>complete</u> structure, the equations of motion can be derived via the Lagrange formulation,

$$\frac{d}{dt} \left(\frac{\partial T}{\partial \dot{u}} \right) - \frac{\partial T}{\partial u} + \frac{\partial U}{\partial u} + \frac{\partial D}{\partial \dot{u}} = \frac{\partial W}{\partial u} \quad , \tag{1}$$

where T and U represent the kinetic and strain energies, respectively, of the <u>complete</u> structure; D is the Rayleigh's dissipation function representing the energy lost in the system due to resisting forces proportional to velocities $\dot{u}$ (e.g. viscous damping forces); and δW represents the virtual work done on the structure by the external forces through virtual displacements δu.

The complete set of degrees of freedom u can be subdivided into N subsets, each containing u^n degrees of freedom for each of the N cyclic sectors. Since any given cyclic sector is 'connected' to adjacent cyclic sectors only on its two sides, u^n satisfies the intersector boundary compatibility condition

$$u^n_{side\ 2} = u^{n+1}_{side\ 1} \quad , \quad n = 1, 2, \ldots, N. \tag{2}$$

Equations (1), therefore, can be written as N sets of equations coupled only as given by equations (2):

$$\frac{d}{dt} \left(\frac{\partial T^n}{\partial \dot{u}^n} \right) - \frac{\partial T^n}{\partial u^n} + \frac{\partial U^n}{\partial u^n} + \frac{\partial D^n}{\partial \dot{u}^n} = \frac{\partial W^n}{\partial u^n} \quad , \quad n = 1, 2, \ldots, N \ . \tag{3}$$

For clarity of presentation, without loss of generality, equations (3) are first applied to obtain the equations of motion of an arbitrary grid point in any cyclic sector by considering its three translational degrees of freedom. Inclusion of the three rotational degrees of freedom at the arbitrary grid point, and extension to include the remaining grid points in the cyclic sector are considered subsequently.

EQUATIONS OF FORCED MOTION

With reference to Figure 1, point P is an arbitrary grid point of the nth cyclic sector with a mass of 'm' units lumped from the adjacent finite elements. Substitution of the expressions for T, U, D and δW in the Lagrange equations (3) results in the following equations of forced motion of point P expressed in the displacement (global) coordinate system A-xyz:

$$[M]\{\ddot{u}\} + \left[[B] + 2\Omega[B_1]\right]\{\dot{u}\} + \left[[K] - \Omega^2[M_1]\right]\{u\} = \{P\} - [M_2]\{\ddot{R}_0\} . \tag{4}$$

The terms appearing in equations (4) are given in Appendix A.

Equations (4) describe the translatory motion of an arbitrary point P in an arbitrary sector n of the rotating cyclic structure subjected to a directly applied vibratory load $\{P\}$ and base acceleration $\{\ddot{R}_0\}$.

These equations can be extended to include the three rotational degrees of freedom at point P by noting that:

1) in a lumped mass model, only the translational degrees of freedom at any grid point contribute to the kinetic energy of the structure, and

2) the coupling between various degrees of freedom may exist only via the stiffness matrix. (Instances where the damping matrix is defined proportional to the stiffness matrix also may result in coupled equations of motion.)

Accordingly, the matrices derived from kinetic energy considerations, $[M]$, $[B_1]$, $[M_1]$ and $[M_2]$ of equation (4) can be expanded as typified by

$$[M]_{6\times6} = \begin{bmatrix} [M_{tt}] & 0 \\ \hline 0 & 0 \end{bmatrix} , \tag{5}$$

where $[M_{tt}]$ is the 3x3 (<u>t</u>ranslational) mass matrix of equation (4). With subscripts t and r representing the <u>t</u>ranslational and <u>r</u>otational degrees of freedom at point P, the stiffness and damping matrices may be expanded as

$$[K] = \begin{bmatrix} [K_{tt}] & \vdots & [K_{tr}] \\ - & - & - \\ [K_{rt}] & \vdots & [K_{rr}] \end{bmatrix} , \tag{6}$$

and

$$[B] = \begin{bmatrix} [B_{tt}] & \vdots & [B_{tr}] \\ - & - & - \\ [B_{rt}] & \vdots & [B_{rr}] \end{bmatrix} . \tag{7}$$

By similar reasoning, the equations of forced vibratory motion of all the cyclic sectors of the total structure can be written as

$$[M^n]\{\ddot{u}^n\} + \left[[B^n] + 2\Omega[B_1^n]\right]\{\dot{u}^n\} + \left[[K^n] - \Omega^2[M_1^n]\right]\{u^n\} = \{P^n\} - [M_2^n]\{\ddot{R}_o\},$$

$$n = 1, 2, \ldots, N. \tag{8}$$

The intersegment boundary compatibility is specified by equation (2).

3. SOLUTION OF EQUATIONS OF MOTION

The method of solution of the equations of forced motion (equations 8 and 2), is based upon the form in which the excitation of the rotating structure is specified. Because of its eventual implementation in the NASTRAN general purpose finite element structural analysis program, the following solution procedure is generally similar to the theoretical presentation of cyclic symmetry given in the NASTRAN Theoretical Manual [8].

METHOD OF SOLUTION

The method of solution of the equations of motion consists of four principal steps:

1) Transformation of applied loads to frequency-dependent circumferential harmonic components.

2) Application of circumferential harmonic-dependent inter-segment compatibility constraints.

3) Solution of frequency-dependent circumferential harmonic components of displacements.

4) Recovery of frequency-dependent response (displacements, stresses, loads, etc.) in various segments of the total structure.

An overall flowchart outlining the solution algorithm is shown in Figure 2. Provision to include the differential stiffness due to the steady loads is also shown.

1. Transformation of Applied Loads

The transformation to frequency-dependent circumferential harmonic components depends on the form in which the excitation is specified by the user.

Details of the five loading conditions considered are as follows:

Directly applied loads (segment-dependent and periodic in time)

If P^n represents a general periodic load on sector n specified as a function of time at M equally spaced instances of time per period (Figure 3), the load at m^{th} time instant can be written as

$$P^{\overset{m}{n}} = P^{\overset{..0}{n}} + \sum_{\ell=1}^{\ell_L} \left[P^{\overset{-\ell c}{n}} \cos(\overline{m-1}\ell b) + P^{\overset{-\ell s}{n}} \sin(\overline{m-1}\ell b) \right] + (-1)^{m-1} P^{\overset{-M/2}{n}} , \quad (9)$$

$$m = 1, 2, \ldots, M ,$$

where $b = 2\pi/M$, $\ell_L = (M-1)/2$ for odd M, $\ell_L = (M-2)/2$ for even M. The last term in equation (9) exists only when M is even. The coefficients $P^{\overset{-"\ell"}{n}}$ ("ℓ" = 0; ℓc, ℓs, $\ell=1, 2, \ldots, \ell_L$; M/2) in equation (9) are independent of time, and are defined by the relations

$$P^{\overset{-0}{n}} = \frac{1}{M} \sum_{m=1}^{M} P^{\overset{m}{n}} , \qquad (\ell = 0) \qquad \text{Part of (10)}$$

-9-

$$\overset{-\ell c}{P}{}^{n} = \frac{2}{M} \sum_{m=1}^{M} \overset{m}{P}{}^{n} \cos(\overline{m-1}\ell b),$$

$$\overset{-\ell s}{P}{}^{n} = \frac{2}{M} \sum_{m=1}^{M} \overset{m}{P}{}^{n} \sin(\overline{m-1}\ell b), \quad \text{and} \qquad \left. \begin{array}{c} (\ell = 1, 2, \ldots, \ell_L) \end{array} \right\} \qquad \left. \begin{array}{c} \\ \\ \end{array} \right\} \text{(10 Contd.)}$$

$$\overset{-M/2}{P}{}^{n} = \frac{1}{M} \sum_{m=1}^{M} (-1)^{m-1} \overset{m}{P}{}^{n} \quad \text{(M even only)} \quad (\ell = M/2).$$

Each of the coefficient vectors $\overset{-"\ell"}{P}{}^{n}$ on the left hand sides of equations (10) can further be expanded in a circumferential (truncated) Fourier series

$$\overset{-"\ell"}{P}{}^{n} = \overset{-"\ell"}{\overline{P}}{}^{0} + \sum_{k=1}^{k_L} \left[\overset{-"\ell"}{\overline{P}}{}^{kc} \cos(\overline{n-1}ka) + \overset{-"\ell"}{\overline{P}}{}^{ks} \sin(\overline{n-1}ka) \right] + (-1)^{n-1} \overset{-"\ell"}{\overline{P}}{}^{N/2},$$

$$(11)$$

where $n = 1, 2, \ldots, N$,

$"\ell" = 0; \ell c, \ell s, \ell = 1, 2, \ldots, \ell_L; M/2$

$a = 2\pi/N$

$k_L \equiv (N-1)/2$ for N odd

$k_L = (N-2)/2$ for N even.

$$\left. \begin{array}{c} \\ \\ \\ \\ \\ \end{array} \right\} \quad (12)$$

The last term in equation (11) exists only when N is even. The Fourier coefficients $\overset{-"\ell"}{\overline{P}}{}^{"k"}$ ($"k" = 0; kc, ks, k = 1, 2, \ldots, k_L; N/2$) in equation (11) do not vary from sector to sector, and are defined by

$$\overset{-"\ell"}{\overline{P}}{}^{0} = \frac{1}{N} \sum_{n=1}^{N} \overset{-"\ell"}{P}{}^{n} \qquad (k = 0)$$

$$\overset{-"\ell"}{\overline{P}}{}^{kc} = \frac{2}{N} \sum_{n=1}^{N} \overset{-"\ell"}{P}{}^{n} \cos(\overline{n-1}ka)$$

$$\qquad\qquad\qquad\qquad (k = 1, 2, \ldots, k_L) \quad \left. \begin{array}{c} \\ \\ \\ \\ \end{array} \right\} \quad (13)$$

$$\overset{-"\ell"}{\overline{P}}{}^{ks} = \frac{2}{N} \sum_{n=1}^{N} \overset{-"\ell"}{P}{}^{n} \sin(\overline{n-1}ka), \quad \text{and}$$

$$\overset{-"\ell"}{\overline{P}}{}^{N/2} = \frac{1}{N} \sum_{n=1}^{N} (-1)^{n-1} \overset{"\ell"}{P}{}^{n} \quad \text{(N even only)} \quad (k = N/2) .$$

The terms $\bar{P}^{-"\ell"}_{"k"}$ ("ℓ" = 0; ℓc, ℓs, ℓ = 1, 2, ..., ℓ_L; M/2 and "k" = 0; kc, ks, k = 1, 2, ..., k_L; N/2) are the <u>transformed</u> frequency-dependent circumferential harmonic components of the directly applied loads $_p\bar{n}^m$ (m = 1, 2, ..., M and n = 1, 2, ..., N).

<u>Directly applied loads (Circumferential harmonic-dependent and periodic in time).</u>

Such loads can be represented as

$$\bar{P}^{m}_{"k"} = \bar{P}^{-0}_{"k"} + \sum_{\ell=1}^{\ell_L} \left[\bar{P}^{-\ell c}_{"k"} \cos(\overline{m-1}\ell b) + \bar{P}^{-\ell s}_{"k"} \sin(\overline{m-1}\ell b) \right] + (-1)^{m-1} \bar{P}^{-M/2}_{"k"} , \quad (14)$$

where m = 1, 2, ..., M represent the time instances at which harmonic components "k" = 0; kc, ks, k = 1, 2, ..., k_L; N/2 of directly applied loads are specified.

The coefficients $\bar{P}^{-"\ell"}_{"k"}$ on the right hand side of equation (14) are obtained using equations (10) with sector number n replaced by harmonic number "k".

<u>Directly applied loads (frequency-and segment-dependent)</u>

This type of loads can be represented as

$$p^{"\ell"}_n = \bar{P}^{-"\ell"}_0 + \sum_{k=1}^{k_L} \left[\bar{P}^{-"\ell"}_{kc} \cos(\overline{n-1}ka) + \bar{P}^{-"\ell"}_{ks} \sin(\overline{n-1}ka) \right] + (-1)^{n-1} \bar{P}^{-"\ell"}_{N/2} , \quad (15)$$

where "ℓ" (=1, 2, ..., F) now represents the frequencies at which excitation is specified. The transformed frequency-dependent circumferential harmonic components $\bar{P}^{-"\ell"}_{"k"}$ ("k" = 0; kc, ks, k = 1, 2, ..., k_L; N/2) are obtained using equations (13) with "ℓ" as defined above.

<u>Directly applied loads (frequency- and circumferential harmonic-dependent)</u>

These loads <u>are</u> the transformed frequency-dependent circumferential harmonic components $\bar{P}^{-"\ell"}_{"k"}$ ("k" = 0; kc, ks, k = 1, 2, ..., k_L; N/2) with "ℓ" (=1, 2, ..., F) representing the various frequencies at which the directly applied loads are specified.

<u>Base acceleration (frequency- and circumferential harmonic-dependent)</u>

In Appendix B, it is shown that the components of the translational base acceleration contribute to inertial loads on the rotating structure in the following manner:

1. Axial component contributes to $\bar{P}^{"k"}_{-"\ell"}$ where "k" = 0, and "ℓ" represents the specified excitation frequencies.

2. Lateral components contribute to $\bar{P}^{"k"}_{-"\ell"}$ where "k" = 1c and 1s, and "ℓ" represents the **effective** excitation frequencies which are shifted from the specified frequencies by $\pm \Omega$, the rotational frequency.

2. Application of Inter-Segment Compatibility Constraints

As shown in Section 4.5.1 of Reference 8, equations (2) are used to derive the compatibility conditions relating the circumferential harmonic component degrees of freedom on the two sides of a rotationally cyclic sector:

<u>side 2</u>   <u>side 1</u>

$$\bar{u}^0_2 = \bar{u}^0_1 \qquad\qquad (k = 0)$$

$$\bar{u}^{kc}_2 = \bar{u}^{kc}_1 \cos(ka) + \bar{u}^{ks}_1 \sin(ka)$$
$$\bar{u}^{ks}_2 = -\bar{u}^{kc}_1 \sin(ka) + \bar{u}^{ks}_1 \cos(ka) \qquad (k = 1, 2, \ldots, k_L)$$

and $\quad \bar{u}^{N/2}_2 = -\bar{u}^{N/2}_1 . \qquad\qquad (k = N/2)$

$$\tag{16}$$

In order to apply these constraint relationships for any given harmonic k, an independent set $\bar{u}^K$ consisting of the circumferential harmonic component (cosine and sine) degrees of freedom from the interior and side 1 of the cyclic sector is defined. $\bar{u}^K$ is selected from the 'analysis' set degrees of freedom (i.e., the degrees of freedom retained after the application of constraints and any other reduction procedures), and is defined as

$$\bar{u}^{kc} = G_{ck}(k)\, \bar{u}^K, \quad \text{and}$$
$$\bar{u}^{ks} = G_{sk}(k)\, \bar{u}^K \qquad .$$

$$\tag{17}$$

$\bar{u}^{kc}$ and $\bar{u}^{ks}$ each contain all (and only) the 'analysis' set degrees of freedom from the interior and **both** sides of the cyclic sector. Equations (16) are used to define some of the elements of the transformation matrices G_{ck} and G_{sk}. For k = o and N/2, the matrix G_{sk} is null.

3. Solution of Frequency-Dependent Harmonic Displacements

For a given harmonic k, the introduction of $\overline{u}^K$ in the equations of motion, equations (8), results in the transformed equations of motion

$$\overline{M}^K \ddot{u}^K + \overline{B}^K \dot{u}^K + \overline{K}^K \overline{u}^K = \overline{P}^K \quad , \tag{18}$$

where
$$\overline{M}^K = G_{ck}^T M^n G_{ck} + G_{sk}^T M^n G_{sk} \, ,$$

$$\overline{B}^K = G_{ck}^T B^n G_{ck} + G_{sk}^T B^n G_{sk} \, ,$$

$$\overline{K}^K = G_{ck}^T K^n G_{ck} + G_{sk}^T K^n G_{sk} \, , \text{ and}$$

$$\overline{P}^K = G_{ck}^T \overline{P}^{kc} + G_{sk}^T \overline{P}^{ks} \, . \tag{19}$$

As discussed earlier, $\overline{P}^{kc}$ and $\overline{P}^{ks}$ are the transformed frequency-dependent circumferential harmonic components of the directly applied and base acceleration loads.

At any excitation frequency ω', let

$$\overline{P}^K = \overline{P}^K e^{i\omega' t} \quad \text{and accordingly,}$$

$$\overline{u}^K = \overline{\overline{u}}^K e^{i\omega' t} \quad , \tag{20}$$

where $\overline{P}^K$ and $\overline{\overline{u}}^K$ are complex quantities. Equation (18) can be rewritten as

$$[-\omega'^2 \overline{M}^K + i\omega' \overline{B}^K + \overline{K}^K] \overline{\overline{u}}^K = \overline{P}^K \quad . \tag{21}$$

The excitation frequency ω' is given by

$$\omega' = \omega \text{ for all directly applied and axial base acceleration loads, and}$$
$$= \omega \pm \Omega \text{ for lateral base acceleration loads.} \tag{22}$$

Equation (21) is solved for $\overline{\overline{u}}^K$ for all excitation frequencies and all harmonics as specified by the user. The cosine and sine harmonic components of displacements are recovered using equations (17).

4. Recovery of Frequency-Dependent Displacements in Various Segments

This step is carried out only when the applied loads are specified on the various segments of the complete structure.

For loads specified as functions of time, equation (11) is used to obtain the displacements $_u n^{-"\ell"}$ in various segments with "ℓ" $= 0$; ℓc, ℓs, $\ell = 1, 2, \ldots, \ell_{max}$. The circumferential harmonic k is varied from k_{min} to k_{max}. The user specifies ℓ_{max}, k_{min} and k_{max}.

For loads specified as functions of frequency, equation (15) is used to obtain the displacements $_u n^{-"\ell"}$ in various segments with "ℓ" representing the excitation frequencies. The circumferential harmonic is varied from user specified k_{min} to k_{max}.

The theoretical development discussed above has been implemented as a new capability in NASTRAN Level 17.7. All aspects of the capability, including DMAP changes, are extensively documented in References 4 and 5.

4. EXAMPLES

Five inter-related examples are presented to illustrate the theoretical development of the previous sections. The new capability added to NASTRAN to conduct forced vibration analysis of rotating cyclic structures [5] has been used to conduct these examples. A 12-bladed disc is used for demonstration.

Example 1 is conducted on a finite element model of the complete structure (Figure 4). Examples 2 through 5 use a finite element model of one rotationally cyclic sector (Figure 5). Results of example 1 are used to verify some of the results obtained in the remaining examples. Table 1 summarizes the principal features of these examples.

Steady-state frequency-dependent (sinusoidal) or time-dependent (periodic) loads are applied to selected grid point degrees of freedom. The specified loads can represent either the physical loads on various segments or their circumferential harmonic components. For illustration purposes only, the frequency band of excitation, 1700-1920 Hz, due to directly applied loads and base acceleration is selected to include the second bending mode of the disc for a circumferential harmonic index $k = 2$. The 'blade-to-blade' distribution of the directly applied loads also corresponds to $k = 2$. Table 2 lists the first few natural frequencies of the bladed disc for $k = 0$, 1 and 2. Modes for $k = 2$ are shown in Figure 7.

GENERAL INPUT

1. Parameters:

Diameter at blade tip	=	19.4 in.
Diameter at blade root	=	14.2 in.
Shaft diameter	=	4.0 in.
Disc thickness	=	0.25 in.
Blade thickness	=	0.125 in.
Young's modulus	=	30.0×10^6 lbf/in^2
Poisson's ratio	=	0.3
Material density	=	7.4×10^{-4} lbf-sec^2/in^4
Uniform structural damping (g)	=	0.02

2. Constraints:

A cylindrical coordinate system with origin at the Basic origin, Z axis along Basic X axis, and θ measured from the Basic Y axis is chosen as the global (displacement) coordinate system for all grid points.

All constraints are applied in <u>body-fixed</u> global coordinate system(s). All grid points on the shaft diameter are completely fixed. Rotational degrees of freedom $\theta_{Z_{cyl}}$ at remaining grid points are constrained to zero.

RESULTS

Figures 8 and 9 present a comparison of grid point displacement and element stresses from examples 1 and 2. The results are seen to be identical from both these examples. The CPU time, however, on IBM 370/3031 was 750 seconds for example 1 as compared to 185 seconds for example 2. The expected behavior about the k = 2 natural frequency of 1814 Hz can be seen in both these figures.

Figures 10 (k = 0), 11 (k = 1c) and 12 (k = 2c) are from example 3. The k = 0 excitation consists of axial base acceleration and directly applied loads. The selected frequency band of excitation, 1700-1920 Hz, lies between the second out-of-plane disc bending mode frequency (1577 Hz, k = 0, Table 2) and the first in-plane shear mode frequency (1994 Hz, k = 0, Table 2). Since the excitation is parallel to the axis of rotation, only the former mode responds. The k = 1 excitation is due to lateral base acceleration only. Although the frequency band of input base acceleration is 1700-1920 Hz, the rotation of the bladed disc at 600 Hz splits the input bandwidth into two effective bandwidths:

(1700 - 600) = <u>1100</u> to (1920 - 600) = <u>1320</u> Hz, and
(1700 + 600) = <u>2300</u> to (1920 + 600) = <u>2520</u> Hz.

The only k = 1 mode in these effective bandwidths is the first torsional mode of the blade with the disc practically stationary (2460 Hz, k = 1, Table 2). This is shown by the out-of-plane displacement magnitudes of grid points 18 (blade) and 8 (disc) respectively (Figure 11). The k = 2 excitation consists of directly applied k = 2c loads. The out-of-plane displacement magnitude of grid point 18 (Figure 12) compares well with that obtained in example 2 (Figure 8). Table 3 lists the out-of-plane displacement response of grid point 18 as obtained in examples 2 and 3. The marginal difference in response in example 3 is due to the Coriolis and centripetal acceleration effects at a rotational speed of 600 revolutions per second.

Results from examples 4 and 5 compare well with th   from example 3, and are shown in Table 4.

5. CONCLUSIONS

1.   Theoretical aspects of a new capability, developed and added to the general purpose finite element program NASTRAN Level 17.7 to conduct forced vibration analysis of tuned cyclic structures rotating about their axis of symmetry, have been presented.

2.   The effects of Coriolis and centripetal accelerations together with those due to the translational acceleration of the axis of rotation have been included.

3.   A variety of user options is provided to specify the loads on the rotating structure.

4.   Five interrelated examples are presented to illustrate the various features of this development.

7. ACKNOWLEDGEMENT

7. REFERENCES

1. Smith, G. C. C., and Elchuri, V., "Aeroelastic and Dynamic Finite Element Analyses of a Bladed Shrouded Disc," Final Technical Report, NASA CR 159728, March 1980.

2. Elchuri, V., Smith, G. C. C., Gallo, A. Michael, and Dale, B. J., "NASTRAN Level 16 Theoretical, User's, Programmer's and Demonstration Manuals Updates for Aeroelastic Analysis of Bladed Discs," NASTRAN Manuals, NASA CR's 159723-159726, March 1980.

3. Gallo, A. Michael, Elchuri, V., and Skalski, S. C., "Bladed-Shrouded-Disc Aeroelastic Analyses: Computer Program Updates in NASTRAN Level 17.7," NASTRAN Manuals, NASA CR 165428, December 1981.

4. Elchuri, V., and Smith, G. C. C., "Finite Element Forced Vibration Analysis of Rotating Cyclic Structures," Final Technical Report, NASA CR 165430, December 1981.

5. Elchuri, V., Gallo, A. Michael, and Skalski, S. C., "Forced Vibration Analysis of Rotating Cyclic Structures in NASTRAN," NASTRAN Manuals, NASA CR 165429, December 1981.

6. Elchuri, V., and Smith, G. C. C., "NASTRAN Flutter Analysis of Advanced Turbopropellers," Final Technical Report, NASA CR 167926, April 1982.

7. Elchuri, V., Gallo, A. Michael, and Skalski, S. C., "NASTRAN Documentation for Flutter Analysis of Advanced Turbopropellers," NASTRAN Manuals, NASA CR 167927, April 1982.

8. <u>NASTRAN Level 17.6 Theoretical Manual</u>, NASA SP 221(05), October 1980.

APPENDIX A

TERMS APPEARING IN EQUATION 4

$$\{u\} = \left\{ \begin{array}{c} u_x \\ u_y \\ u_z \end{array} \right\} \tag{A1}$$

$$\{P\} = \left\{ \begin{array}{c} P_x \\ P_y \\ P_z \end{array} \right\} \tag{A2}$$

$$\{\ddot{R}_0\} = \left\{ \begin{array}{c} \ddot{X}_0 \\ \ddot{Y}_0 \\ \ddot{Z}_0 \end{array} \right\} \tag{A3}$$

$$[M] = [M]^{global} = [T^{GB}]^T \begin{bmatrix} m & 0 & 0 \\ 0 & m & 0 \\ 0 & 0 & m \end{bmatrix} [T^{GB}] \tag{A4}$$

$$[B] = [B]^{global} \tag{A5}$$

$$[B_1] = [B_1]^{global} = [T^{GB}]^T \begin{bmatrix} 0 & 0 & 0 \\ 0 & 0 & -m \\ 0 & m & 0 \end{bmatrix} [T^{GB}] \tag{A6}$$

$$[K] = [K]^{global} \quad \text{(includes all differential stiffness contributions)} \tag{A7}$$

$$[M_1] = [M_1]^{global} = [T^{GB}]^T \begin{bmatrix} 0 & 0 & 0 \\ 0 & m & 0 \\ 0 & 0 & m \end{bmatrix} [T^{GB}] \tag{A8}$$

$$[M_2] = [T^{GB}]^T \begin{bmatrix} m & 0 & 0 \\ 0 & mc & ms \\ 0 & -ms & mc \end{bmatrix} \tag{A9}$$

$$c \equiv \cos \Omega t \quad , \quad s \equiv \sin \Omega t \quad , \text{ and} \tag{A10}$$

$$\begin{Bmatrix} \hat{\imath} \\ \hat{\jmath} \\ \hat{k} \end{Bmatrix} = [T^{BG}] \begin{Bmatrix} \hat{I}_B \\ \hat{J}_B \\ \hat{R}_B \end{Bmatrix} \quad . \tag{A11}$$

APPENDIX B

INERTIAL LOADS DUE TO BASE ACCELERATION

The acceleration of the axis of rotation generates inertial loads at all grid points of the complete structure. In this appendix, the generation of these inertial loads and their transformation to frequency-dependent circumferential harmonic components are discussed.

As given by equation (4), the inertial forces on the three translational degrees of freedom at an arbitrary point P of the modelled cyclic sector, expressed in the global (displacement) coordinate system, are

$$\{P^G\} = -[M_2]\{\ddot{R}_0\} = [T^{BG}]\{P^B\} \quad , \tag{B1}$$

where

$$\{P^B\} = \begin{Bmatrix} P_X \\ P_Y \\ P_Z \end{Bmatrix}^B = -\begin{bmatrix} m & 0 & 0 \\ 0 & m & 0 \\ 0 & 0 & m \end{bmatrix}\begin{bmatrix} 1 & 0 & 0 \\ 0 & c & s \\ 0 & -s & c \end{bmatrix}\begin{Bmatrix} \ddot{X}_0 \\ \ddot{Y}_0 \\ \ddot{Z}_0 \end{Bmatrix} \quad , \tag{B2}$$

with $c \equiv \cos \Omega t$ and $s \equiv \sin \Omega t$.

Since all the cyclic sectors are identical in all respects except for the specified loads, no generality is lost in assuming, for simplicity, that the modelled sector is the $n = 1$ sector. Equation (B1) can, then, be rewritten as

$$\{P^G\} = [T^{BG}]\begin{bmatrix} 1 & 0 & 0 \\ 0 & c_n & s_n \\ 0 & -s_n & c_n \end{bmatrix}\{P^B\} \tag{B3}$$

where

$$\left.\begin{aligned} c_n &= \cos(\overline{n-1} \cdot 1 \cdot 2\pi/N), \quad \text{and} \\ s_n &= \sin(\overline{n-1} \cdot 1 \cdot 2\pi/N) \quad . \end{aligned}\right\} \tag{B4}$$

Substituting equation (B3) in equations (13), and noting that

$$\sum_{n=1}^{N} c_n \equiv 0 \tag{B5}$$

$$\sum_n s_n \equiv 0$$

$$\sum_n c_n \cdot \cos(\overline{n-1} \cdot k \cdot 2\pi/N) = N/2 \quad , \quad k=1$$
$$= 0 \quad , \quad k \neq 1 \quad ,$$

$$\sum_n s_n \cdot \cos(\overline{n-1} \cdot k \cdot 2\pi/N) \equiv 0 \quad ,$$

$$\left.\begin{array}{l}\end{array}\right\}$$ (B5)
(contd)

$$\sum_n c_n \cdot \sin(\overline{n-1} \cdot k \cdot 2\pi/N) \equiv 0 \quad ,$$

$$\sum_n s_n \cdot \sin(\overline{n-1} \cdot k \cdot 2\pi/N) = N/2 \quad , \quad k=1$$
$$= 0 \quad , \quad k \neq 1 \quad ,$$

the circumferential harmonic components of the base acceleration loads become

$$\{\overline{P}^0\}^G = [T^{BG}] \left\{\begin{array}{c} P_X \\ 0 \\ 0 \end{array}\right\}^B \quad , \quad (\text{"k"} = 0)$$

$$\{\overline{P}^{1c}\}^G = [T^{BG}] \left\{\begin{array}{c} 0 \\ P_y \\ P_z \end{array}\right\}^B \quad , \quad (\text{"k"} = 1c)$$

$$\left.\begin{array}{l}\end{array}\right\}$$ (B6)

$$\{\overline{P}^{1s}\}^G = [T^{BG}] \left\{\begin{array}{c} 0 \\ P_Z \\ -P_Y \end{array}\right\}^B \quad , \quad (\text{"k"} = 1s) \text{ , and}$$

$$\{\overline{P}^{kc,ks}\}^G = \{0\} \quad , \quad \text{all other "k".}$$

In the present development, the components of base acceleration $\ddot{X}_0$, $\ddot{Y}_0$ and $\ddot{Z}_0$ are considered to be sinusoidal of frequency ω, and are specified as

$$\ddot{X}_0 = \ddot{X}_{0,\text{mag}} \cos(\omega t + \phi_X) \quad ,$$

$$\ddot{Y}_0 = \ddot{Y}_{0,\text{mag}} \cos(\omega t + \phi_Y) \text{ , and}$$

$$\left.\begin{array}{l}\end{array}\right\}$$ (B7)

$$\ddot{Z}_0 = \ddot{Z}_{0,\text{mag}} \cos(\omega t + \phi_Z) \quad .$$

From equation (B2) therefore, we can write

$$P_X^B = -m\ddot{X}_{0,mag.} \cos(\omega t + \phi_X) \quad ,$$

$$P_Y^B = -m[\ddot{Y}_{0,mag} \cos \Omega t \cdot \cos(\omega t + \phi_Y) + \ddot{Z}_{0,mag} \sin \Omega t \cdot \cos(\omega t + \phi_Z)], \text{ and}$$

$$P_Z^B = -m[-\ddot{Y}_{0,mag} \sin \Omega t \cdot \cos(\omega t + \phi_Y) + \ddot{Z}_{0,mag} \cos \Omega t \cdot \cos(\omega t + \phi_Z)]. \quad \text{(B8)}$$

The cosine and sine products in equations (B8) can be expressed in terms of individual cosine and sine terms with frequencies $(\omega + \Omega)$ and $(\omega - \Omega)$.

The following conclusions about base acceleration loads can, therefore, be drawn by substituting equations (B8) into equations (B6):

1. The axial component of base acceleration, $\ddot{X}_0(\omega)$, contributes to $\bar{P}^0$ at excitation frequencies ω.

2. The lateral components of base acceleration, $\ddot{Y}_0(\omega)$ and $\ddot{Z}_0(\omega)$, contribute to $\bar{P}^{1c}$ and $\bar{P}^{1s}$ at excitation frequencies $(\omega \pm \Omega)$ for each ω specified.

NOMENCLATURE

B	Damping matrix
B_1	Coriolis acceleration coefficient matrix
D	Rayleigh's dissipation function
G	"Symmetric Components" transformation matrix
$\hat{I}, \hat{J}, \hat{K}$	Unit vectors along Inertial XYZ axes
$\hat{I}_B, \hat{J}_B, \hat{K}_B$	Unit vectors along Basic X_B Y_B Z_B axes } (Figure 1)
$\hat{i}, \hat{j}, \hat{k}$	Unit vectors along Global xyz axes
K	Stiffness matrix
k	Circumferential harmonic index
ℓ	Time harmonic index
M	Mass matrix, number of time intervals per period (Figure 3)
M_1	Centripetal acceleration coefficient matrix
M_2	Base acceleration coefficient matrix
m	Mass
N	Number of cyclic sectors in the complete structure
P	Load vector
Q	Aerodynamic coefficient matrix
$\ddot{R}_0$	Base acceleration vector
$\vec{r}, \vec{R}, \vec{\rho}$	Position vectors (Figure 1)
T	Kinetic energy, coordinate system transformation matrix
t	Time
U	Strain energy
u	Physical displacement degrees of freedom
W	Virtual work
Ω	Rotational frequency
ω	Forcing frequency

NOMENCLATURE (Continued)

Superscripts

B ·	Basic
G	Global
K	Independent solution set in "symmetric components"
m	mth time instant
n	nth cyclic sector

$$
\left.\begin{array}{l}
-0 \\
-\ell c \\
-\ell s \\
-kc \\
-ks \\
-M/2 \\
-N/2
\end{array}\right\} \quad \text{Fourier coefficients ("symmetric components")}
$$

NOTE: The above superscripts have been used in the paper to qualify various scalars, vectors and matrices, such as T, U, u, P, M, K. They should not be confused with exponents.

$\vec{I}, \vec{J}, \vec{K}$ Unit vectors along Inertial XYZ axes

$\vec{i}_B, \vec{j}_B, \vec{k}_B$ Unit vectors along Basic $X_B Y_B Z_B$ axes

$\vec{i}, \vec{j}, \vec{k}$ Unit vectors along Global xyz axes
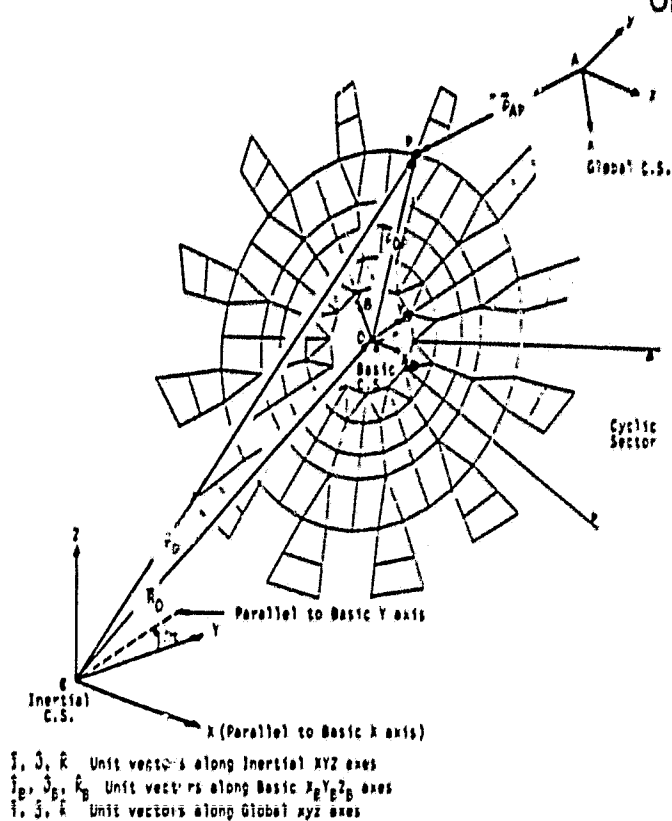
Figure 1: Coordinate Systems
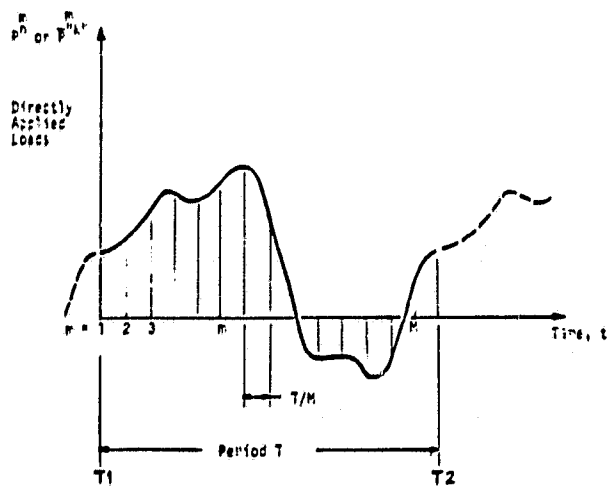
Figure 3: Directly Applied Periodic Loads Specified as Functions of Time
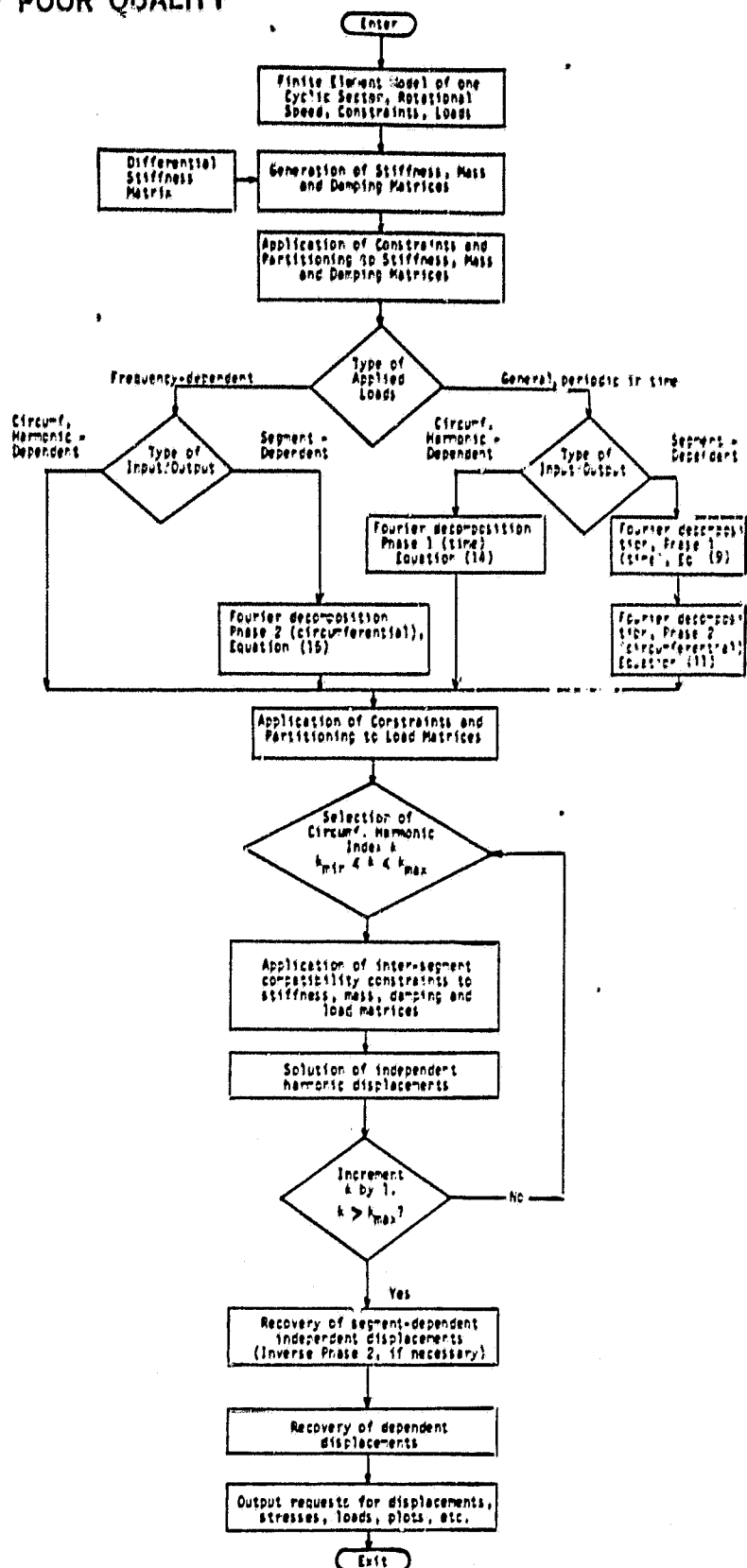
FIGURE 2: Overall Flowchart of Forced Vibration Analysis of Rotating Cyclic Structures
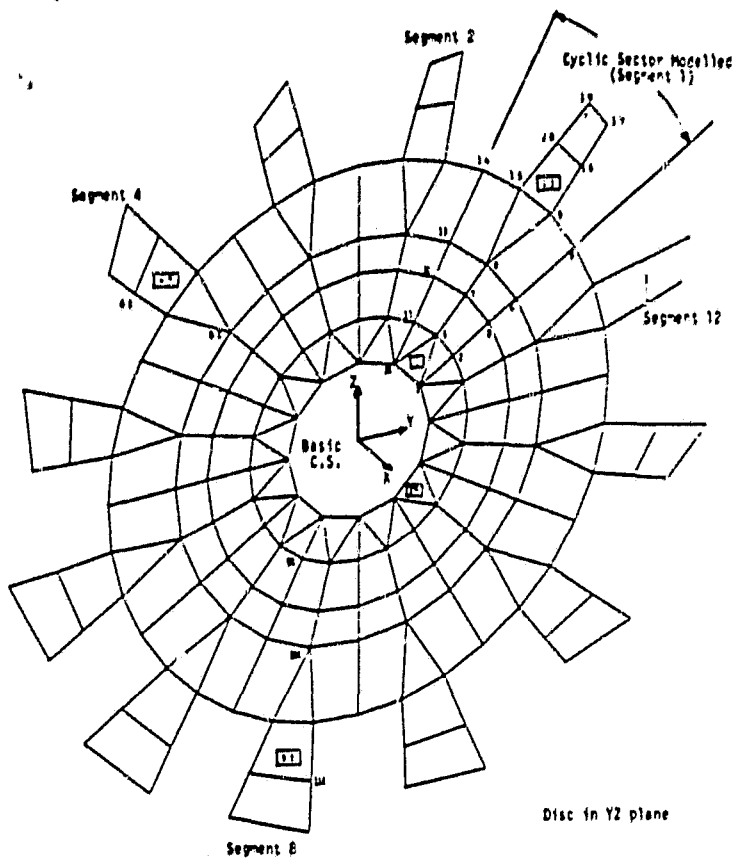
Figure 4: NASTRAN Model of the 12-Bladed Disc (Plate Elements)
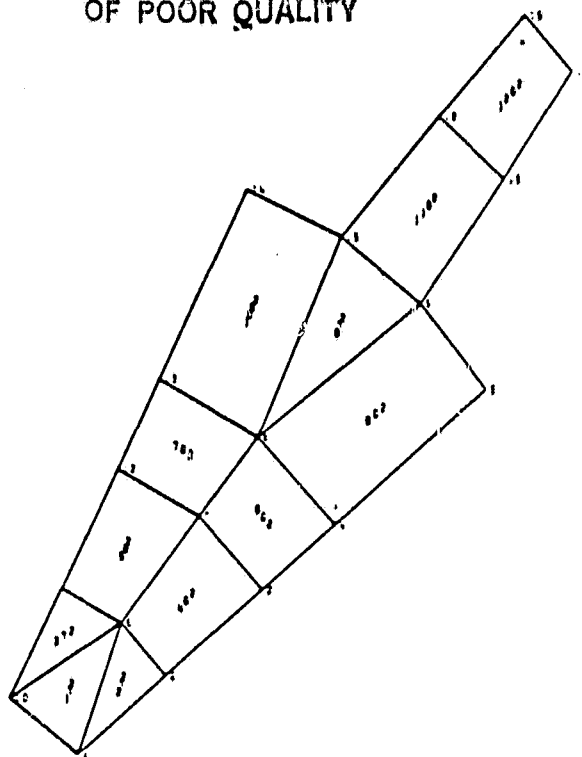
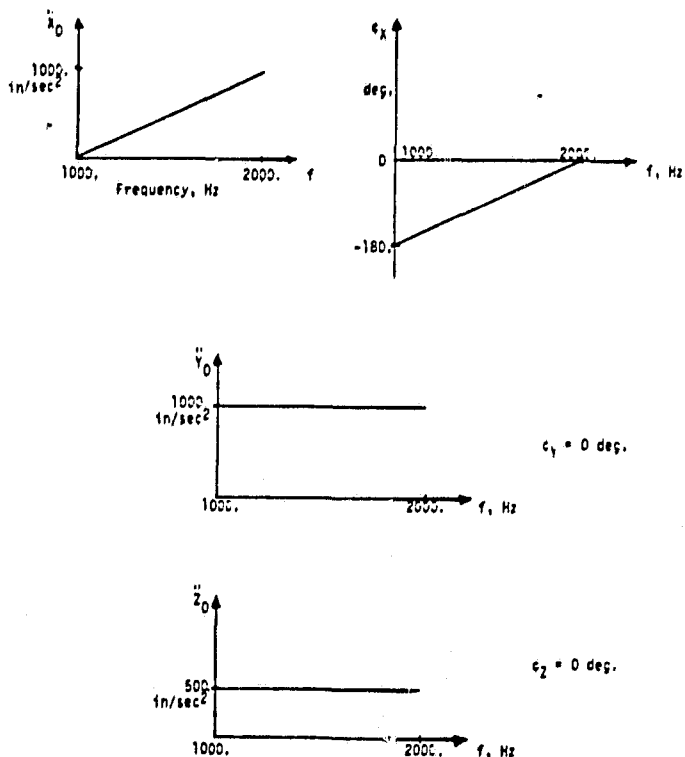Figure 5: NASTRAN Cyclic Model of the 12-Bladed Disc (Plate Elements)

Figure 6: Base Acceleration Data in an Inertial Coordinate System
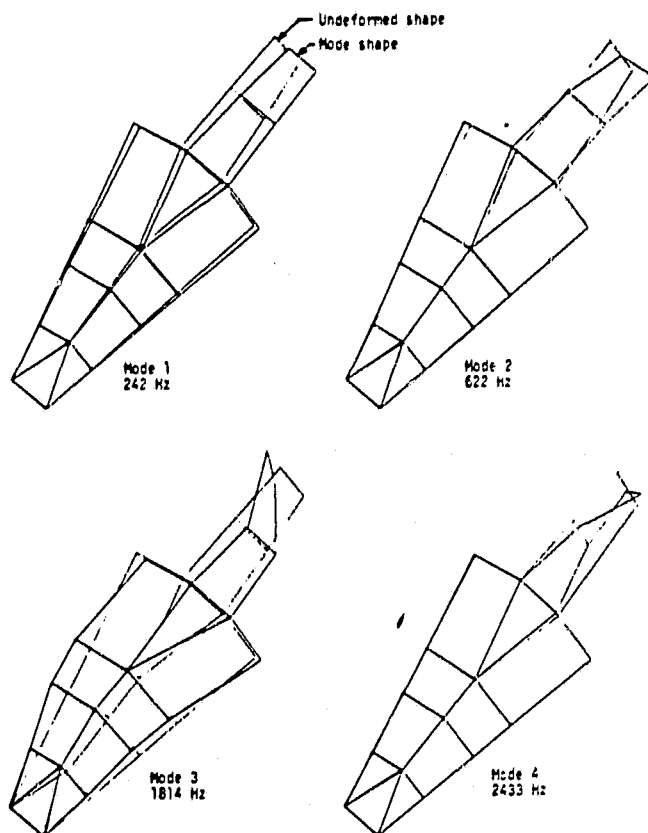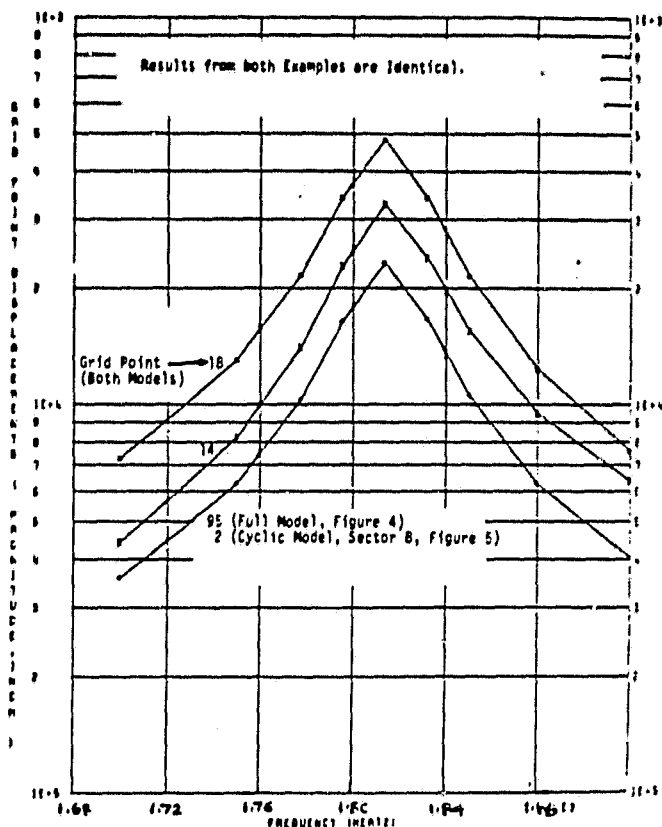

Figure 7: k = 2 Modes of Bladed Disc

Figure 8: Comparison of Z_{cyl} Displacements from Example 1 (Full Model)
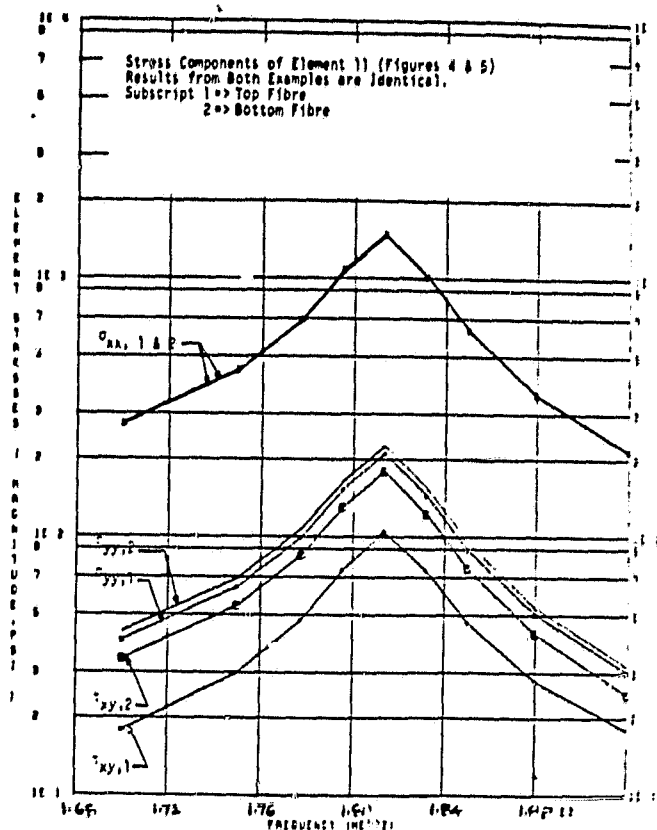and Example 2 (Cyclic Model)

Figure 9: Comparison of Element Stress Components from Example 1 (Full Model)
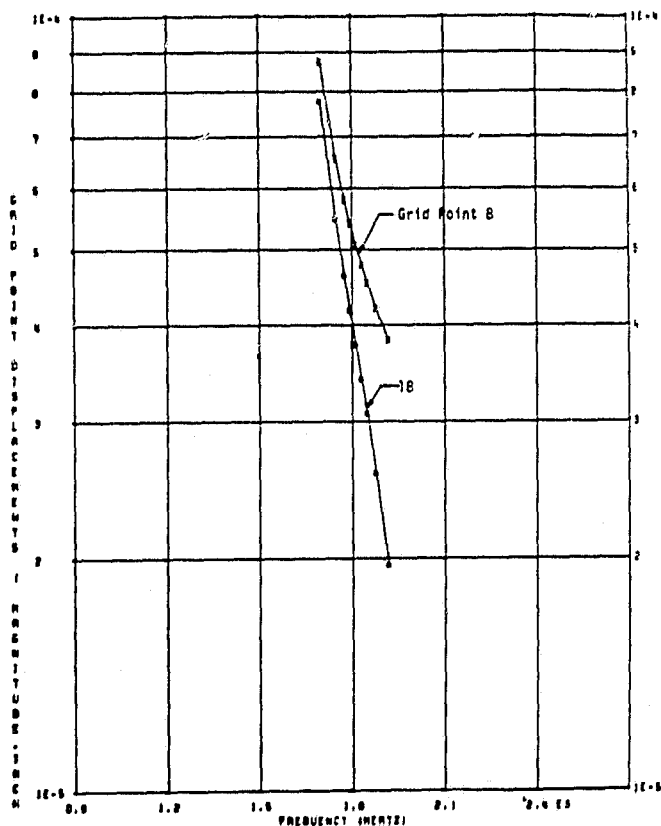and Example 2 (Cyclic Model)

Figure 10: Z_{cyl} Displacements from Example 3, k = 0, Directly Applied
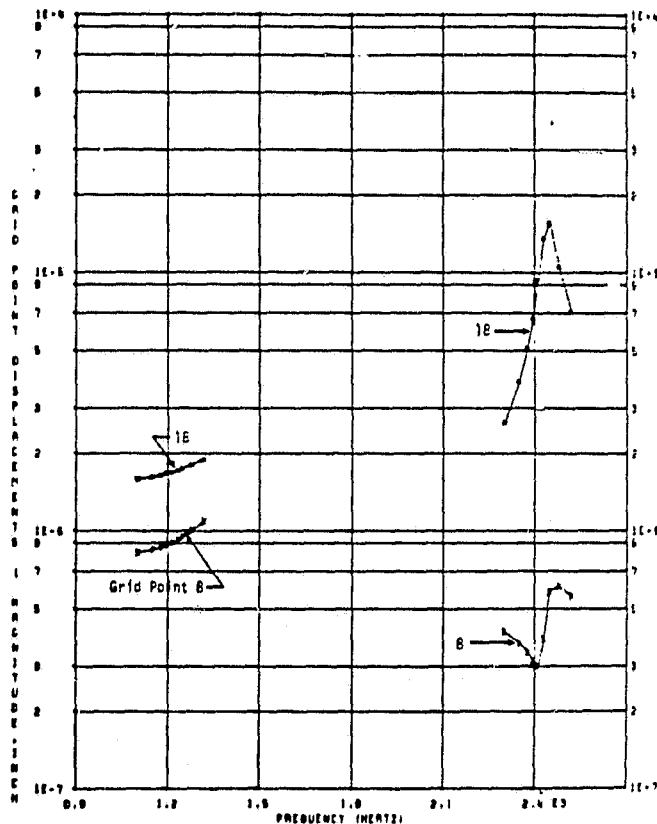and Axial Base Acceleration Loads

Figure 11: Z_{cyl} Displacements from Example 3, k = 1c, Lateral Base
Acceleration Loads

TABLE 1: PRINCIPAL FEATURES OF EXAMPLE PROBLEMS

Example No.	Finite Element Model of	Applied loads specified as functions of				Base Acceleration	Rotational Speed
		Frequency (sinusoidal)		Time (periodic)			
		Physical Components	Circum. Harmonic Components	Physical Components	Circum. Harmonic Components		
1	Complete Structure	A					
2	Cyclic Sector	B					
3	Cyclic Sector		C			Figure 6	600 rps
4	Cyclic Sector			D			600 rps
5	Cyclic Sector				E		600 rps

NOTES:
A. $P(f,n) = A(f) \cdot \cos(\overline{n \cdot T} \cdot 2 \cdot 2\pi/12)$
B. $P^n(f) = A(f) \cdot \cos(\overline{n \cdot T} \cdot 2 \cdot 2\pi/12)$
C. $\overline{P}^0, \overline{P}^{2c} = A(f)$
D. $P^n(t) = A(t) \cdot \cos(\overline{n \cdot T} \cdot 2 \cdot 2\pi/12)$
E. $\overline{P}^{2c} = A(t)$

F.

Grid pt./DOF	A(f)	A(t)/sin(2···1814·t)
B/Z_{cyl}	-1	-1
16/Z_{cyl}	1	1
18/Z_{cyl}	1	1

TABLE 3: EFFECT OF CORIOLIS AND CENTRIPETAL ACCELERATIONS ON THE DISPLACEMENT RESPONSE OF GRID POINT 18 AT 600 RPS.

Frequency Hz	Example 2 — Segment 1 Mag. (in)/Phase (deg)	Example 3 — k = 2c Mag. (in)/Phase (deg)
1700	7.2655 E-5/349.4	7.6132 E-5/354.3
1750	1.3071 E-4/343.1	1.3844 E-4/347.3
1778	2.1580 E-4/332.7	2.3252 E-4/335.8
1796	3.4139 E-4/314.6	3.7252 E-4/315.2
1814	4.8374 E-4/269.9	4.9177 E-4/266.6
1832	3.4143 E-4/224.9	3.2655 E-4/225.5
1850	2.1451 E-4/206.6	2.0742 E-4/209.3
1880	1.2433 E-4/195.6	1.2214 E-4/199.2
1920	7.6125 E-5/190.4	7.5397 E-5/194.3

TABLE 2: BLADED-DISC NATURAL FREQUENCIES

| Frequency (Mode No.), Hz			Mode Description
k = 0	k = 1	k = 2	
214 (1)	208 (1)	242 (1)	
591 (2)	594 (2)	622 (2)	
1577 (3)	1633 (3)	1814 (3)	
2466 (5)**	2460 (4)	2433 (4)	

* k is the circumferential harmonic index

** Mode No. 4 for k = 0 at 1994 Hz represents an in-plane shear mode not excited by the applied forces.

TABLE 4: COMPARISON OF RESPONSE AT 1814 Hz.

Grid Pt.Disp. or Elem. Stresses	Example 3 — k = 2c Mag. (in)/Phase (deg)	Example 4 — Segment 1 Mag. (in)/Phase (deg)	Example 5 — k = 2c Mag. (in)/Phase (deg)
B (Z_{cyl})	5.4297 E-4/82.6	5.4295 E-4/82.6	5.4295 E-4/82.6
18 (Z_{cyl})	4.9177 E-4/266.8	4.9180 E-4/266.8	4.9180 E-4/266.8
11, $\sigma_{xx,1}$*	1.4841 E 3/84.7	1.4?? E 3/84.7	1.4542 E3/84.7
11, $\sigma_{yy,1}$	2.0891 E 2/83.4	2.0892 E 2/83.4	2.0893 E2/83.4
11, $\tau_{xy,1}$	1.0774 E 2/64.7	1.0775 E 2/64.7	1.0775 E2/64.7
11, $\sigma_{xx,2}$*	1.4677 E 3/263.3	1.4678 E3/263.3	1.4678 E3/263.3
11, $\sigma_{yy,2}$	2.2489 E 2/260.3	2.2491 E 2/260.4	2.2491 E3/260.4
11, $\tau_{xy,2}$	1.8510 E 2/253.0	1.8511 E 2/253.0	1.8512 E2 253.0

* Top and Bottom Fibres.
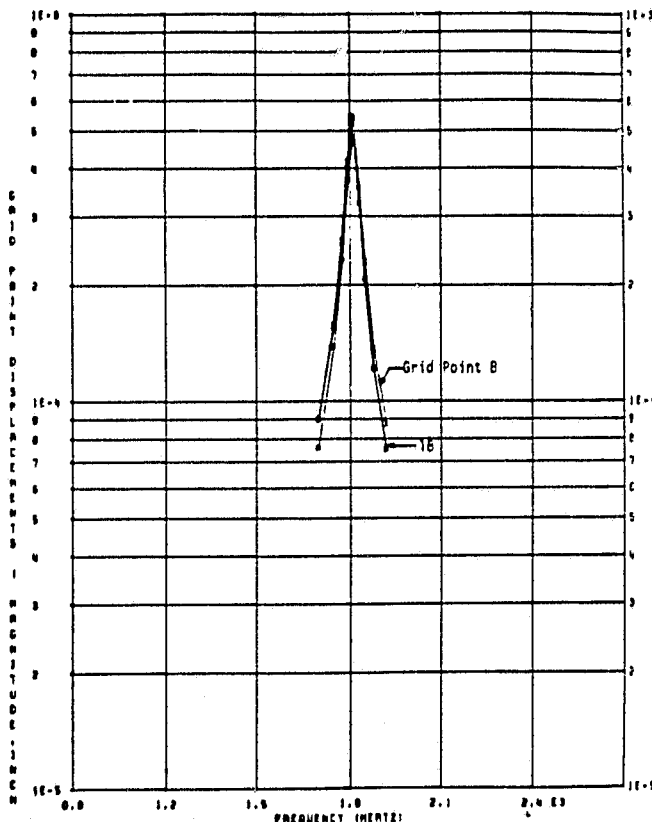
Figure 12: Z_{cyl}. Displacements from Example 3, k = 2c, Directly Applied Loads